Chapter 3
Principles of Induction Accelerators

Richard J. Briggs

3.1 Introduction

The basic concepts involved in induction accelerators are introduced in this chapter. The objective is to provide a foundation for the more detailed coverage of key technology elements and specific applications in the following chapters. A wide variety of induction accelerators are discussed in the following chapters, from the high current linear electron accelerator configurations that have been the main focus of the original developments, to circular configurations like the ion synchrotrons that are the subject of more recent research. The main focus in the present chapter is on the induction module containing the magnetic core that plays the role of a transformer in coupling the pulsed power from the modulator to the charged particle beam. This is the essential common element in all these induction accelerators, and an understanding of the basic processes involved in its operation is the main objective of this chapter. (See [1] for a useful and complementary presentation of the basic principles in induction linacs.)

3.2 Basic Features of an Induction Accelerator System

As described in the historical summary in the previous chapter, linear induction accelerators were originally developed to fill a need for higher charged particle energies than a single stage diode could provide, at pulse currents beyond the capability of RF accelerators. The multistage induction accelerator configurations developed to accelerate particles to these higher energies are similar in overall appearance to the more common RF linac. In an induction accelerator module, however, as we describe in more detail in this chapter, the pulsed power source is directly coupled to the beam through a low impedance structure, the *induction cell*. This induction cell plays the same role as the resonant cavities used in RF accelerators. It is more

R.J. Briggs (Retired) (✉)
SAIC, Alamo, CA, USA; SSCL, Dallas, TX, USA; LLNL, Livermore, CA, USA
e-mail: richardbriggs@sbcglobal.net

K. Takayama, R.J. Briggs (eds.), *Induction Accelerators*, Particle Acceleration and Detection, DOI 10.1007/978-3-642-13917-8_3,

appropriate for accelerating high beam currents and/or providing general (non-sinusoidal) acceleration waveforms since the accelerating voltage comes directly from the pulse modulator.

Induction accelerators can be thought of in simple terms as a series of 1:1 transformers where pulsed voltage sources form the transformer primary circuit and the charged particle beam pulse acts as the secondary (as illustrated by the cartoon in Fig. 3.1). The rise time (τ_r), fall time (τ_f), and duration (τ_p) of a typical source voltage pulse (see Fig. 3.2) and the beam current pulse are generally in the range of tens of nanoseconds to several microseconds. In these cases the transit time of electromagnetic waves over the dimensions of a typical accelerator cell (fractions of a meter) are short compared to these characteristic pulse times. The electromagnetic fields in the accelerator cell can then generally be modeled in a quasi-static approximation. As a consequence, lumped circuit models of the accelerator module are often very useful approximations, as we show in the following sections.

A key point about this multistage accelerator module configuration as compared to single stage pulsed diodes is the fact that the peak voltages on drive cables, vacuum insulators, and other elements in the system are limited to the output of the pulse source driving one module. The charged particles, in effect, do the integration of the axial electric field in the vacuum beam pipe to achieve a final energy equal to the sum of all the individual module voltages. The *total* voltage corresponding

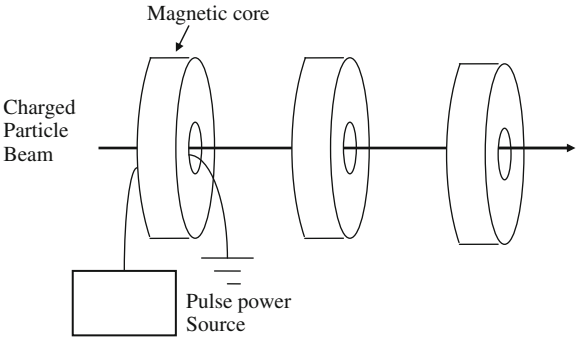

Fig. 3.1 Induction accelerator as a series of 1:1 transformers

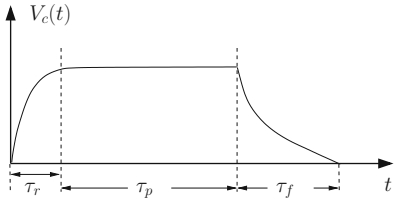

Fig. 3.2 Typical source voltage waveform applied to primary of induction core for constant acceleration over the pulse duration (τ_p). More complex waveforms can also be used as discussed in the following chapters

to the sum of the individual module voltages doesn't appear on physical structures anywhere in the system, even if the voltage pulse length is much longer than the transit time of electromagnetic waves, or particles, through the entire system.

The basic functional elements that make up an induction accelerator system are the following.

1. The *induction cell* that couples the electromagnetic energy to the charged particle beam. This cell contains the magnetic core material that acts as the transformer. It must also provide the vacuum barrier (an insulator structure) between the evacuated beam line transporting the charged particles and the rest of the system. The basic physical processes involved in its operation are discussed in Sect. 3.3. A detailed discussion of the magnetic material properties of the core is covered in Chap. 5.
2. The *pulse power system* that delivers the pulsed voltage (accelerating electric field) to the accelerating gap in the cell. These systems are discussed in Chap. 4. Depending on the specific application, the pulsed power system can range from very low rep rates (single shot) to very high rep rates.
3. An *injector* including a charged particle source that creates the charged particle beam pulse (in a linac system). Injectors for high current electron beam applications are discussed in Chap. 7, while Chap. 9 covers ion sources for induction linacs.
4. A *focusing system* to transport the charged particle beam through the accelerator cells, similar to those used in RF linacs and synchrotrons. In linear accelerators, the magnetic elements of this transport system (solenoids, quads) are often integrated into the cell to economize on axial space and achieve the highest possible acceleration gradient. Focusing systems for high current electron beam induction linacs are discussed in Chap. 7, while some aspects of focusing systems for ion induction linacs are discussed in Sect. 10.1.5.

The design of an induction module, consisting of an induction cell and the pulsed power system that drives it, often involves a number of tradeoffs. These tradeoffs and other design considerations are discussed in Chap. 6, using a number of examples from accelerators that have actually been constructed and operated.

In addition to these hardware elements, the *beam transport and beam-cell interaction* are key physics issues in the design of an induction accelerator. Indeed, as discussed in Chap. 6, in high current applications minimization of the transverse and/or longitudinal interaction impedance of the accelerator module (the "wake fields") often dominates various parameter choices (like the gap width and the beam pipe diameter).

In typical electron linear induction accelerators, the particles are highly relativistic right out of the injector. The defocusing from the radial electric field created by the beam space charge is canceled to a high degree by the azimuthal magnetic field created by the beam current (within $1/\gamma^2$, where γ is the electron energy in rest mass units). As a consequence, the design of the transverse focusing system for a high current relativistic electron induction linac is generally dominated by control of coherent *transverse* instabilities (beam breakup and image displacement

instabilities described in Chap. 7), rather than the basic considerations of particle optics and available aperture.

In contrast, in the high current, high brightness ion induction accelerators discussed in Chaps. 9 and 10, the design of the focusing systems are generally dominated by consideration of the basic particle optics in the presence of strong radial space charge forces. Instability concerns are more often dominated by the *longitudinal* dynamics and the longitudinal interaction impedance that controls it, when the particles are only mildly relativistic.

In the induction synchrotrons discussed in Chaps. 11 and 12, the beam currents are much lower than in induction linacs but the repetition rates of the power systems are much higher. The transverse beam focusing systems are basically unchanged in the conversion from RF power systems to induction systems. Many novel aspects of the longitudinal dynamics are encountered, however, as discussed in these chapters.

3.3 Comparison Between RF Accelerators and Induction Accelerators

For readers familiar with RF accelerators [2], a discussion of the comparisons between RF accelerators and induction accelerators might be helpful at this point. Readers without any background in RF accelerators should probably skip this section until they have read the subsequent two sections in this chapter.

A typical linear induction accelerator has identical modules adding an increment of energy to the charged particle beam, as described in Sect. 3.2. This basic configuration is very similar in appearance to the more common radio frequency accelerator. The features that distinguish the two technologies can be describes in several different ways, from several different points of view.

From the perspective of the charged particle beam being accelerated: In an RF accelerator, a short "micro-bunch" passes through successive acceleration modules (or makes repetitive trips through the same module in a synchrotron) carefully timed to match a given phase of the sinusoidally varying acceleration "voltage" (axial electric field) waveform. A series of these "micro bunches" is typically used to form much longer duration "macro-bunches" (or DC particle currents). Any axial focusing of the micro-bunch that is required can be automatically provided by locating the bunch on a sloping part of the sinusoidal waveform rather than the peak of the voltage.

In an induction accelerator the beam pulse length is typically several orders of magnitude longer than the charged particle transit time through an individual module. The accelerating electric field in the region of the accelerating gap and inside the beam pipe is essentially quasi-static in character. The basic acceleration voltage waveform is also most often a flat-topped pulse. In electron induction linacs, no axial focusing is required. In ion induction linacs or induction synchrotrons, "ear pulses" or "barrier pulses" at the ends of the bunch might be provided by

tailoring the induction module pulsed power drive pulse, or by using separate modules designed for that function.

From the perspective of the power coupling to the beam: An essential role of the high Q resonant cavities in RF accelerators is to provide a large transformer step-up ratio. That is, the high Q cavity provides an impedance match between the relatively low impedance of the RF (or microwave) transmission lines feeding energy into the cavity (10's – 100's of ohms) loaded by a relatively high (typically mega-ohm class) "beam impedance" (beam voltage gain per module divided by the beam current). The electromagnetic energy is stored in the cavity for times the order of Q/ω.

The induction cell, as already noted, is a non-resonant (low Q) structure containing a magnetic core that basically serves as a 1:1 isolating auto-transformer. This allows the modulators to drive the beam current directly and be summed to any energy using a series of modules. The electromagnetic energy from the pulsed power sources flow directly into the beam without being stored in the cell. With multi-kilo-Amp charged particle beam pulses, and cell voltages of several hundred kilovolts, the beam impedance in high current linac systems often provides a reasonable match when coupled directly to the pulsed power sources and their transmission line feeds. The induction accelerator in these situations can operate at relatively high efficiencies as discussed in more detail in Chap. 6.

From the perspective of the accelerator cell voltage gradient and wake impedances: High Q RF cavities can provide relatively high acceleration gradients per watt of source drive power. At the same time, the high Q cavity does make the suppression of transverse and longitudinal instabilities more of an issue in high beam current applications.

Induction accelerators generally have a lower acceleration gradient than RF accelerators. The "packaging" issues, vacuum insulator voltage stress limits, and volt-second limitations in the magnetic core material are all important constraints particularly for pulse durations of order a microsecond or longer. The non-resonant character of the cell itself, however, does facilitate reductions in the wake field impedances to very low values by insertion of damping elements at strategic locations.

Considering these basic differences we see that the induction approach is, in general, more suitable for the acceleration of high beam currents with relatively long ("micro-bunch") pulse lengths compared to RF accelerators. Indeed, as the discussion in the previous chapter illustrated, the primary motivation for the early development of multistage linear induction accelerators for electrons was the achievement of high instantaneous beam currents, from hundreds to thousands of Amps, in pulse lengths ranging from tens of nanoseconds to several microseconds. For some applications, like radiography of fast processes, this combination of current and pulse length comes from the requirement for a high charge per pulse to make a sufficient radiation dose, in a pulse length less than the dynamic timescale of the process (e.g., like 50–100 ns). Multistage accelerators, as opposed to single stage diode configurations, are necessary, or perhaps favored, when the required particle energy is high, and/or the beam quality requirement is demanding.

The flexibility in the acceleration waveform is another attribute of induction acceleration that motivates its use in various ion accelerators, as indicated above and discussed in more detail in the following chapters, even when the beam current is low enough for RF acceleration to be used.

3.4 Physical Processes Inside a Typical Induction Module

To illustrate the basic physical processes in an induction module, a cutaway view of an induction cell like those used in the electron linear accelerators built in the 1970s and 1980s at LLNL and LBNL is shown in Fig. 3.3.

A voltage pulse generated by the pulsed power system (for example, by switching stored energy out of a charged transmission line or PFN) is transmitted to the induction module through a balanced set of coaxial lines as shown. Symmetrical drives through two (or more) lines are generally used to avoid deflection forces on the beam from multi-kilo-Amp drive currents.

In the presence of a charged particle beam moving down the axis and being accelerated, a return current I_B flows in the beam pipe wall and up the gap as shown in Fig. 3.3. The beam current will therefore appear as a load on the drive transmission lines connecting the pulsed power source to the cell.

A fundamental design objective in all induction accelerator systems is to have the cylindrical magnetic core present a relatively high impedance to the drive

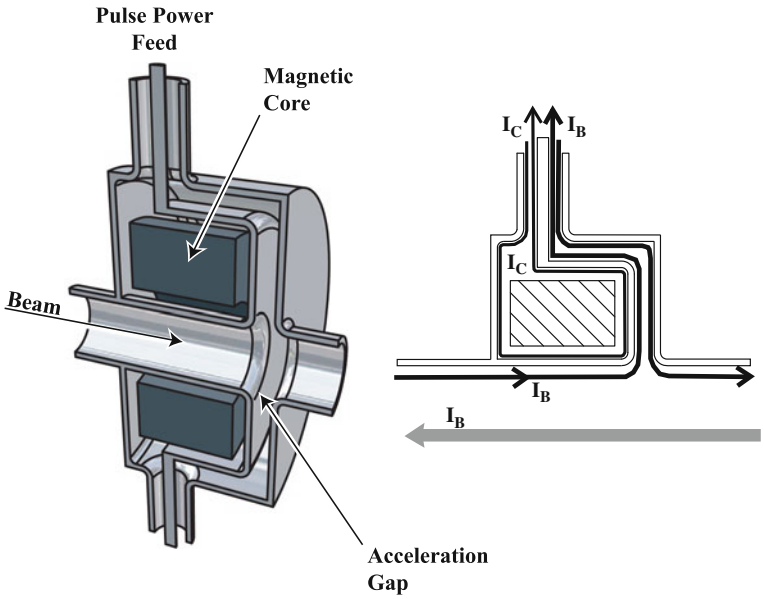

Fig. 3.3 Cutaway view of induction cell and the current flow during the pulse flat top in an induction module (the direction of the beam current is illustrated for electrons)

transmission lines and the pulsed power source to minimize the "magnetizing current" I_c flowing into the core region (shown in Fig. 3.3). In high current induction accelerators, a key metric for how well the design meets this objective is a comparison of the magnetizing current with the beam current. As discussed in Chap. 6, when multi-kilo-Amp beams are accelerated, the magnetizing current can be made a small fraction of the total drive current resulting in high energy transfer efficiency. In all cases, however, minimization of the magnetizing current is desirable to minimize core losses and to simplify the compensation of voltage "droop" from this nonlinear, rate dependent load.

It is implicit in this picture that the beam and voltage pulse durations (and rise and fall times) are long compared to the electromagnetic propagation time through the radial gap structure so that the fields can be treated in a quasi-static approximation. Note in particular that the electric field in the vicinity of the accelerating gap is quasi-static in character, as illustrated in the sketch in Fig. 3.4. There is no electromagnetic coupling between the modules as long as the beam pipe length between successive gaps is longer than the evanescent decay length of the quasi-static electric field (one or two beam pipe radii). Note also that all the charged particles passing through the gap region gain V_c electron volts independent of their trajectory or distance from the axis, in the same way as having a DC voltage across the gap. In the rise time and fall time of the voltage pulse, the charging (and discharging) of the gap voltage leads to a displacement current flowing through the feed line to the cell, in addition to the currents I_c and I_B indicated in Fig. 3.3.

The circuit schematic presented in Fig. 3.5 that follows from these physical considerations can be used for zero-order modeling of the accelerator module operation. Note that the beam current load on the drive transmission line is accurately represented as a current source in this equivalent circuit, since this load current is not dependent on the voltage of that stage as it would be in a diode. A gap capacitance C_g has also been added to this simple circuit model to account for the displacement current flow during the rise time and fall time transients discussed above.

The magnetic core is represented in the schematic by an equivalent load impedance Z_c. This core load is nonlinear and rate dependent (dispersive), as we discuss in the following subsection, so that the relationship between the cell voltage and the time dependent "magnetizing current" I_c is quite complicated in general.

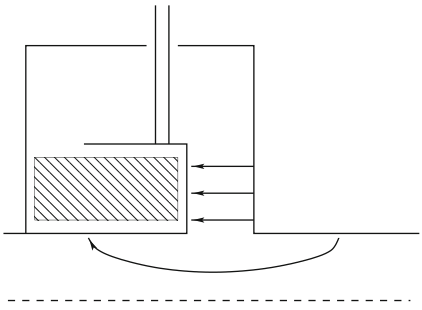

Fig. 3.4 Sketch of the electric field in the gap region and inside the beam pipe

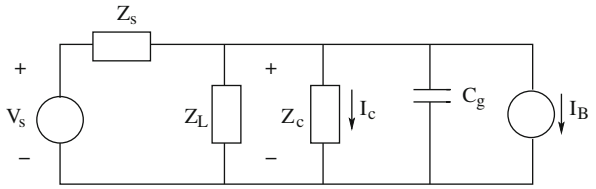

Fig. 3.5 Simplified circuit schematic of induction unit. The pulsed power source (including any transmission line cables that connect it to the cell) is represented by an equivalent voltage source V_s and series impedance Z_s. External compensation circuits at the cell junction are represented by the impedance Z_L. The core impedance (nonlinear in general) is Z_c, the gap capacitance is C_g, and the time dependent beam current load is the current source I_B

When the nonlinearities are not dominating the response (early times in the pulse and/or operation at lower amplitudes), the core impedance of ferromagnetic laminated cores can often be adequately represented by a parallel L-R circuit. The core inductance can be estimated from small amplitude permeability measurements, and the parallel resistance value chosen to reproduce the core losses for the magnetization rates of interest.

The pulsed power source is represented in the schematic by a voltage generator V_s with internal impedance Z_s as shown. An external compensation circuit with an impedance Z_L is also included in the schematic. In most induction accelerators this network is placed in an external oil filled (to provide-high voltage insulation) box and connected across the drive line just outside the induction module. This external load can be used to help flatten the acceleration voltage pulse, compensating for the rise time transients and time-dependent core currents, and also to absorb energy when the beam is absent (i.e., suppress ringing in the drive transmission lines and possible voltage doubling).

To illustrate the usefulness of this equivalent circuit in the design and operation of an induction accelerator, let us consider a simple case where the magnetic core impedance is very high ($I_c \simeq 0$), and the source and compensation load impedances are purely resistive. With the simple "step function" source voltage of amplitude V_0 and pulse duration τ_0 as illustrated in Fig. 3.6a, the cell voltage rise time is limited by the cell capacitance. Without any beam loading the cell voltage prior to the end of the pulse is given by

$$V_c(t) = V_{co}[1 - \exp(-t/\tau_R)], \tag{3.1}$$

where

$$\begin{aligned} V_{co} &= \left(\frac{Z_L}{Z_L + Z_S}\right) V_0, \\ \tau_R &= R_{\text{net}} C_g, \\ R_{\text{net}} &= \frac{Z_L Z_s}{Z_L + Z_s}. \end{aligned} \tag{3.2}$$

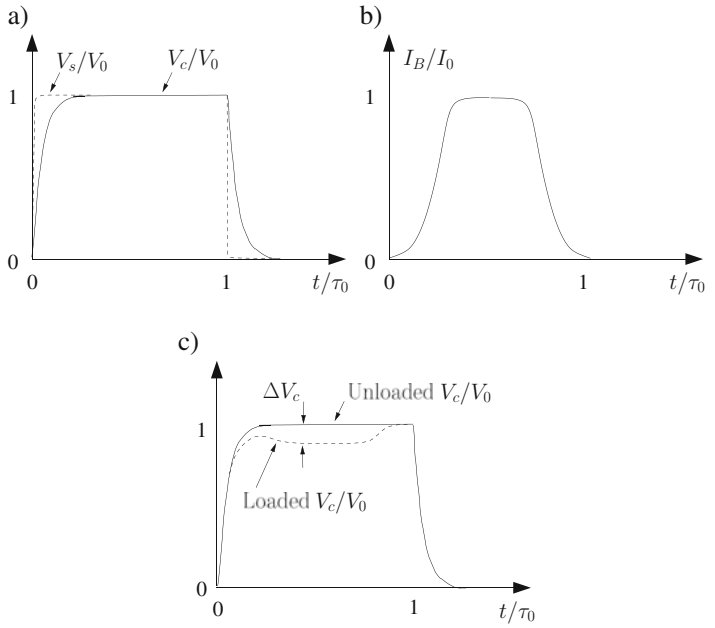

Fig. 3.6 Illustration of (**a**) time dependent cell voltages in a simple case, (**b**) beam current pulse example, and (**c**) cell voltage waveform with beam current loading (assumed to be 20%) compared with the unloaded cell voltage waveform

This cell voltage waveform is also sketched in Fig. 3.6a for the case when the rise time (and fall time) τ_R is equal to about 5% of the total pulse length.

If a beam pulse of duration less than the source voltage pulse and peak amplitude I_0 passes through the cell, as sketched in Fig. 3.6b, the cell voltage would have the form indicated in Fig. 3.6c. This cell voltage waveform is easily derived by superposition of the response to each of the two sources, V_s and I_B. The "loading" by the beam drops the cell voltage by an amount

$$\Delta V = R_{\text{net}} I_0 \tag{3.3}$$

in the flat top region of the waveform. (In Fig. 3.6c it is assumed that this loading is 20%). The power into the beam in the flat top region is therefore

$$V_c I_B = \left(\frac{Z_L}{Z_L + Z_s} \right) (V_0 - Z_s I_0) I_0. \tag{3.4}$$

With a given source impedance and source voltage, as a function of beam current the maximum energy transfer is obtained when $I_B = V_s/2Z_s$.

It is apparent from the cell voltage sketches in Fig. 3.6 that it is difficult to avoid significant beam energy variations on the head and tail of the beam pulse in a heavily loaded (efficient) induction accelerator driven by simple pulse forming line (PFL) or

pulse forming network (PFN) sources. Compensating for a time-varying beam load current is possible in principle but difficult in practice with these drive systems. This objective might be easier to achieve with modern ("programmable") solid state drive systems.

The equivalent circuit also illustrates that the module voltage rise time is controlled by the product of the gap capacitance and the parallel combination of the source impedance and the compensation circuit impedance. Minimization of this gap capacitance is often an important consideration in the design of short pulse induction accelerators to achieve a fast enough voltage rise time. However, as discussed in Chap. 6, the gap spacing has upper limits because of transverse instability (BBU) considerations.

3.5 Magnetic Core Considerations

The basic function of the magnetic core in an induction cell is to serve as a 1:1 isolating auto-transformer so that each individual modulator can be grounded in the voltage summing process. In addition, as we emphasized in Sect. 3.4, the core should present a relatively high impedance to the drive system so that the power from the modulator flows primarily into the beam and not into the core region.

Let $\Phi(t)$ represent the total azimuthal magnetic flux in the magnetic core located inside the induction module, illustrated in Fig. 3.3. From Faraday's law, this total magnetic flux must change in time to maintain the accelerating voltage, so that

$$\Delta\Phi(t) = \int_0^t V_c(t')\,\mathrm{d}t' \tag{3.5}$$

where we take $t = 0$ as the time when the cell voltage begins. The magnetic flux is the integral of the azimuthal induction field over the core cross section,

$$\Phi = \int B_\theta(r, z, t)\,\mathrm{d}A. \tag{3.6}$$

To predict the magnetizing current I_c flowing into the core region (illustrated in Fig. 3.3) and the time-dependent "impedance" of the core, we need to know the B–H relationship of the magnetic core material. As we discuss in an elementary way in this chapter (as an prelude to the more complete discussions in Chap. 5), the electromagnetic properties of typical magnetic materials used in induction cores are very complicated to describe and to model. Their response is nonlinear, exhibiting hysteresis, and rate dependent (dispersive), as illustrated in the sample B–H relation in Fig. 3.7. It is perhaps surprising that a "zero-order" design of the induction module can be done with only limited modeling of the detailed space-time dependence of the electromagnetic fields in the magnetic material. The objective in the design, once again, is to make all these "complications" as irrelevant as possible,

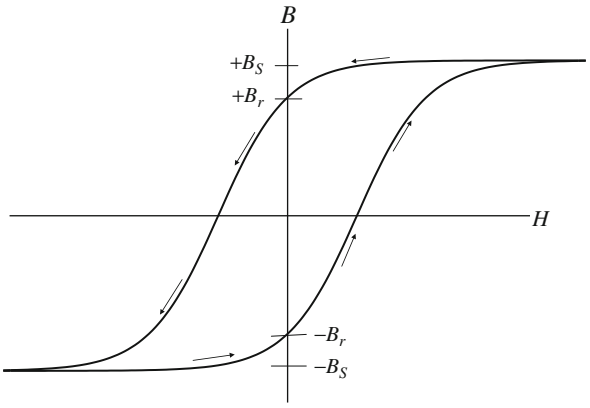

Fig. 3.7 Illustration of nonlinear B–H relation for a typical magnetic core material going from saturation at $-B_s$ to saturation at $+B_s$. The shape of this "trajectory" in B–H space depends on the rate of change of the magnetic flux

by ensuring that the magnetizing current remains as small a perturbation as possible for the full duration of the acceleration voltage pulse. At a minimum, the magnetic core impedance should be as large as possible compared to the pulsed power driver impedance for reasonable waveform control.

The main constraint on the choice of magnetic material and the required volume of material follows from Eq. (3.5). When the voltage pulse is first applied, we assume the core has been reset to $-B_r$. (Circuitry for ensuring this reset occurs is discussed in Chap. 6). During the voltage pulse, the magnetic induction field at any given position will start moving from $-B_r$ towards $+B_s$ (saturation). The details of how various regions of the core move towards saturation can be complicated, since the H field varies throughout the core; we discuss some of these aspects in the following discussions of ferrite and tape wound cores. It is clear, independent of these details, that the product of the pulse voltage and pulse length is limited by the "volt-seconds" product of the core, i.e.,

$$\int V_c \, \mathrm{d}t \ \sim \text{Average}[V_c]\tau_p \leq \Delta B A_c \text{ volt-s}, \tag{3.7}$$

where A_c is the cross sectional area of the core and ΔB is the total flux swing available ($B_r + B_s$ with the assumed reset to $-B_r$). When this volt-s limitation is reached, and all the regions of the core are saturated (i.e., the magnetic flux is on the upper flat part of the B–H curve), the impedance of the core collapses and I_c rapidly rises.

We must also ensure, that the impedance of the core *prior* to saturation is large compared to the pulsed power driver impedance. This constraint is generally satisfied when the volt-second constraint is satisfied, as long as we chose magnetic core material with a relatively high effective permeability prior to saturation.

Equation (3.7), together with other considerations like the magnetization rate and the rep rate (average power and heating), constitute the zero order basis for the choice of magnetic material and the specification of the volume of core material. Examples of how these choices were made in the design of several induction accelerators that were built and operated are discussed in Chaps. 5 and 6.

The details of the space-time dependence of the nonlinear magnetics with a given cell aspect ratio ultimately determine the time dependence and magnitude of the magnetizing current, of course. Compensation for this magnetizing current with networks in the drive circuitry and/or the compensation box are often required to achieve adequate flat top on the module voltage pulse, as can be predicted from the equivalent circuit in Fig. 3.5. In practice the design and "tuning" of these networks are generally done empirically.

One area where the details of the nonlinear magnetics can be important is in the distribution of electrical stresses in the core region. This phenomenology is very different with ferrite magnetic material or tape wound cores, as we discuss below.

3.6 Ferromagnetic Laminated Cores

For long pulse induction accelerators, the large flux swings available with ferromagnetic materials like nickel-iron, silicon steel, and amorphous magnetic material makes their use compelling. Ferromagnetic materials are those in which magnetization is produced by cooperative action between domains of collectively oriented molecules yielding a higher flux density and permeability [3, 4]. However, the conductivity of these materials is many orders of magnitude higher than the ferrites. Basically they are conductors so that it is necessary to manufacture the cores by wrapping thin ribbons (10–40 μm thick) of the material with electrical insulation between the layers to avoid excessive eddy current losses. This is the same technique used to manufacture 50–60 Hz power transformers with this material where the thickness of the laminations can be much greater since the frequency is much lower.

With a laminated core inside an induction cell, the azimuthal H field in the core region is quasi-static and proportional to the magnetizing current. It penetrates "instantly" throughout the insulating layers in the core region since these insulating layers suppress any (bulk) radial currents that would shield it from the core region interior. As we discuss in more detail in Chap. 6, however, the micro-picture of the magnetic field penetration does involve partial shielding of the magnetic flux from the ribbon interiors because of local eddy currents circulating around each ribbon. If the rate of rise of the magnetizing current is slow enough, so that the ribbon thickness is small compared to an equivalent skin depth, this shielding effect and the associated eddy current losses are a small perturbation. In this case, the core impedance one can use in the equivalent circuit in Fig. 3.5 (prior to saturation) is simply the low frequency inductance of the core. This inductance should use the effective rate dependent permeability, for an improved estimate, and a resistor in

parallel to model the losses. The magnetizing current with a flat topped drive voltage pulse, then, will increase linearly in time.

A major difference in the construction of laminated cores for induction cells as opposed to 60 Hz transformers is the requirement for much better layer to layer insulation, as well as thinner ribbons to reduce eddy current losses. With magnetization rates of many Tesla per microsecond, the layer to layer voltages can be tens of volts in the induction cell application as opposed to a millivolt or less in the 60 Hz case, where no additional insulation is required except for the surface discontinuity insulation. The distribution of the pulsed voltages throughout the induction cell is in fact a much more complicated problem than it would first appear; this issue is discussed in detail in Sect. 6.9.

3.7 Ferrites

For pulse lengths much less than a microsecond, the volt-second requirements are more modest and the use of ferrimagnetic materials like ferrite can become attractive. Ferrimagnetic materials are those in which spontaneous magnetic polarization occurs in non equivalent sub-lattices; the polarization in one sub-lattice is aligned anti-parallel to the other yielding a lower flux density and permeability [3, 4]. However, the resistivity of Ni–Zn ferrite is very high ($\sim 10^4 \Omega$-m typically) so that the equivalent skin depth is many meters at the frequencies of interest. The losses of the ferrite material in induction cell applications are dominated by the magnetic losses associated with the spin resonance, as discussed in Chap. 5. Spin resonance absorption at microwave frequencies is similar in principle to nuclear and electronic spin resonance [5]. The magnetic moment of the material precesses about the direction of the static magnetic field and energy is absorbed strongly from a transverse radio frequency field when its frequency is equal to the precessional frequency. At this frequency, the permeability shows an increase and above this frequency the real part of the permeability decreases while the imaginary or lossy part increases.

At frequencies well below the spin resonance, the (small amplitude) permeability can be quite high (several hundred to thousands). This relatively high permeability, together with a dielectric constant of order 10 in typical ferrites, means that the basic electromagnetic propagation speed in ferrite is of order 1% of the speed of light in vacuum. In contrast to all the other regions in an induction cell, therefore, where the electromagnetic fields are quasi-static in character, the ferrite core region will generally involve wave propagation dynamics for an adequate description [1]. The wave amplitudes are generally too large for a linear model of the ferrite to be an adequate description, however.

Induction cell designs using ferrite cores are therefore basically ferrite loaded transmission lines. In later generation designs it was recognized that the wave propagation dynamics in the ferrite could be used to advantage to make the core impedance resistive and also to remain relatively constant throughout the entire duration of the drive voltage pulse. This constant core impedance feature is desirable

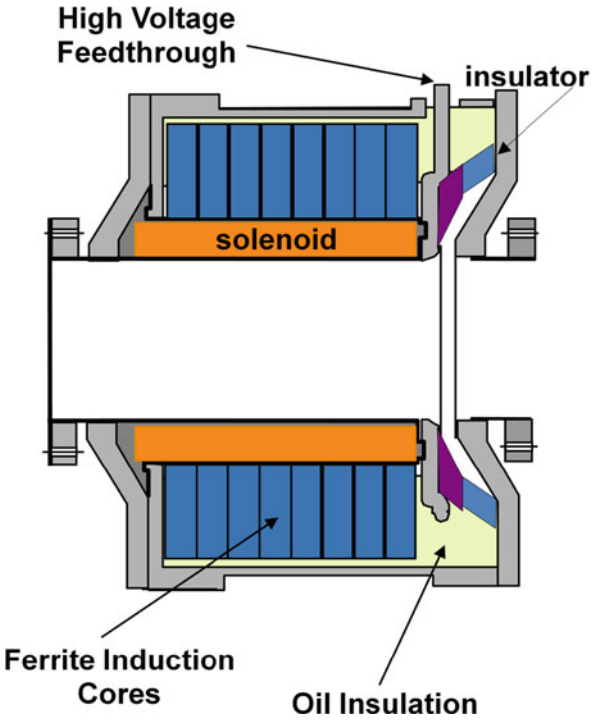

Fig. 3.8 ETA-II induction cell

because it greatly simplifies the compensation requirements to achieve a constant acceleration voltage.

The ETA-II induction cell pictured in Fig. 3.8 illustrates how this feature can be optimized in the cell design as discussed more fully in Sect. 6.2. The 20 cm long coaxial ferrite induction core in ETA-II was driven from one end at the acceleration gap. The two-way propagation time of small amplitude voltages in this line is of order 120–140 ns, slightly longer than the actual pulse length. At the normal operating voltages in ETA-II, the ferrite is driven into saturation and the propagation of the "saturation wave" through the ferrite core cannot be treated adequately as a small amplitude wave. Nonetheless, the measured core impedance in ETA-II up to saturation of the entire core did remain roughly constant at around 200 Ω [6]. This constant core impedance in ETA-II was in marked contrast to the ATA configuration where the drive was applied at the outer radius of the ferrite toroid.

References

1. S. Humphries. *Principles of Charged Particle Acceleration*, Wiley, New York, NY, 1986.
2. T. Wangler. *RF Linear Accelerators*, Wiley, New York, NY, 1998.
3. D. Gray, editor. *American Institute of Physics Handbook*, McGraw-Hill, New York, NY, 1972. see Sect. 5–4.

4. A. Deckker, editor. *Electrical Engineering Materials*, Prentice Hall, New Jersey, 1959. page 96.
5. C. Kittel. *Introduction to Solid State Physics*, Wiley, New York, NY, 8th edition, 2005. see page 363.
6. W. Turner, G. Caporaso, G. Craig, J. De Ford, L. Reginato, S. Sampayan, R. Kuenning, and I. Smith. Impedance Characteristics of Induction Accelerator Cells. In *Proceedings of the 7th International Conference on High-Power Particle Beams*, page 845, Karlsruhe, Germany, 4–8 July 1988.